Front-end of a Non-Invasive Wireless Real-Time Brain Imaging System Based on Near-Infrared Spectroreflectometry

Frédéric Normandin[1], Mohamad Sawan[1], Jocelyn Faubert[2]
[1]PolySTIM Neurotechnology Laboratory, École Polytechnique de Montréal,
Dept. of Electrical Engineering, Montréal, Québec, Canada.
[2]Visual Psychophysics and Perception Laboratory, Université de Montréal, Québec, Canada.
frederic.normandin@polymtl.ca, mohamad.sawan@polymtl.ca, jocelyn.faubert@umontreal.ca

Abstract

In this paper, we present a fully integrated front-end of a portable spectroreflectometry-based brain imaging system dedicated for acquisition of modulated optical signals at a frequency of 50 kHz. The proposed front-end preamplifier is composed of a photodetector, a transimpedance preamplifier, a two-stage voltage amplifier and a mixer. Strict constraints regarding noise thus have to be considered. The preamplifier consists of a transimpedance block featuring a 95 dBΩ gain and an average input current noise density at the frequency of interest of approximately 1 pA/$\sqrt{\mathrm{Hz}}$. Each of the two subsequent voltage amplifiers allows the user to obtain an additional 25 dB gain, which makes it possible to obtain a considerable total gain. Considering the tuning capabilities and the losses due to the filters and the non-ideal buffers, the proposed front-end allows us to obtain a total gain up to 165 dB. The back-end of the amplification chain, is composed of a mixer which is used to produce a continuous voltage proportional to the amplitude of the input optical signals. All those features were integrated using CMOS 0.18 µm technology.

Key words — *Photodiode, transimpedance amplifier, optical receiver, CMOS, spectroreflectometry, brain imaging.*

1. Introduction

IT is important for psychophysicists, neuropsychologists and physicians to monitor, in real-time, the brain activity of a patient. This information is useful for diagnosing cerebral damage or pathologies.

One way to retrieve such information from the cerebral cortex is to use the spectroreflectometry technique. It is based on the measurement of the variation of optical parameters within the brain, such as absorption, diffusion and propagation delay. Previous work has been done on this subject with success. Although the results are very promising for bedside use, there is some difficulty adapting these techniques for portable applications needed for long-term observation or for monitoring the brain during activities involving free movement. For example, [1] proposed a powerful, but bulky time domain tomography spectroreflectometer. Also, a Japanese company, Hamamatsu, offers a series of frequency domain optical imaging systems, again for bedside use.

In this paper, we present the design of a new fully integrated front-end for a portable near-infrared continuous wave spectroreflectometry based imaging system. We will describe the design and CMOS implementation of the proposed system. Post-layout simulation results and a discussion will follow.

2. The Integrated Front-End

The biomedical application of this system is the real-time detection of the activation of the various cortical regions of the human brain. It has already been proven that the detection is possible using an optical network composed of near-infrared emitters and detectors [2].

The complete proposed system is integrated on a small number of CMOS chips because it must not disturb the person under observation by its weight, its connections or its power dissipation. Emitters and receivers are placed non-invasively on the surface of the scalp of the subject

The proposed front-end involves 50 kHz modulated optical signals in the near infrared (NIR) region (700–950 nm). A block diagram of the complete front-end system is illustrated in figure 1.

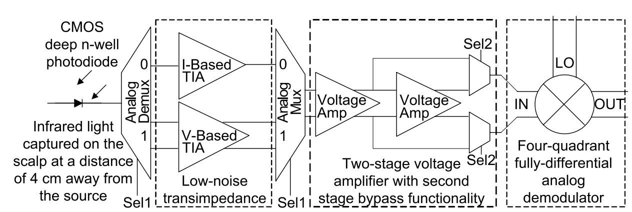

Fig. 1. Front-end for infrared brain imaging system

The first module is the photodetector, a photodiode. The second module is a low noise transimpedance amplifier. This amplifier converts the current generated by the photodetector into voltage signal strong enough to be handled by subsequent amplifier stages. The third module is a two-stage fully differential voltage amplifier. This module is used to amplify even more the voltage signal towards the millivolts range to make it available for external use. The last module is a fully differential analog mixer used for demodulation of the signal.

2.1. Photodiode

Photonic-electronic conversion is made using a silicon photodetector. For good detector dimensioning, the optical power involved in this application has been carefully evaluated by simulation using the MCML software [3], a frequently used application for modeling electromagnetic wave propagation in living tissue. The model used is composed of the five principal light absorbing and diffusing layers of tissue: scalp, skull, CSL, gray matter and white matter. Typical values of the optical parameters of the various layers needed by the simulator, such as refraction index (n), absorption coefficient (μ_a), diffusion coefficient (μ_s) and anisotropy coefficient (g), were taken from literature [4-5]. The results of these simulations indicated that reflectance, i.e. the light retrodiffused towards the outside of cranium after having penetrated it, is 3.73 X 10^{-4} cm^{-2} at a distance of 4 cm of the light source on the surface of the skull. It is at this distance that measurements must be taken to obtain a good reading at the depth of the cerebral cortex [2]. It is thus necessary to take into account this strong optical attenuation for the realization of the receiver.

As the process used is TSMC CMOS 0.18 µm, there are few techniques available for the realization of a photodiode. The choices are: using the junctions between the diffusions and the substrate, the implantations and the substrate or the implantations and the diffusions. Since the wavelengths to be collected are in the NIR band, it is of primary importance to choose the deeper junction available so that the absorbed photons generate electron-hole pairs in the depletion region of the diode. Indeed, at these wavelengths, the length of absorption in silicon is in the order of several microns.

Thus, the chosen junction is the one between the substrate and a deep n-well diffusion. In order to determine the dimensions of the diode, photon generated current must be evaluated by the following equation [6]:

$$I_{ph} = \frac{qP_{abs}}{h\nu} = q\frac{\lambda P_{abs}}{hc} = qA\frac{\lambda p_{disp}}{hc}, \tag{1}$$

where q is the electron charge, P_{abs} is the total optical power absorbed by the detector, A is the detector area, p_{disp} is the power density available to the detector, ν is the light frequency, λ is the absorbed wavelength, h is the Planck constant and c is the light speed.

The light source used in our application emits an optical power of 10 mW. At the detection point, the received power is 3.73 $\mu W/cm^2$ taking into account reflectance given before. Using equation (1) and the one giving the leakage current in a reverse-biased diode, one obtains that a detector area of about 0.5 mm^2 is necessary in order to respect a signal-to-noise of 40 dB needed in this application. Indeed, simulations showed that for the considered wavelengths and this sensor dimensions, the generated photocurrent is in the interval of [11, 14] nA, while the intensity of the leakage current is around 10 pA on the full range of reverse biasing (0 V to 1.8 V). If it is considered that the losses due to the coupling and quantum yield can reduce the generated current by a factor 10, we find a 40 dB ratio between the generated photocurrent and the diode leakage current.

Given the large dimensions (0.7 mm x 0.7 mm) of the photodiode, its surface has been strewn with slits through the well in order to create a substrate contact elsewhere than in periphery of the photodiode. The path that the electron-hole pairs must travel to join the contact and thus to contribute to the photocurrent can be shortened using this technique. In this way, the time of transit of the generated charges is decreased. Moreover, this technique has the advantage of appreciably increasing the surface of the depletion region.

2.2. Low-Noise Transimpedance Preamplifier

The preamplifier is the first stage of the amplification chain of the signal provided by the photodiode. Its role is to convert this current into voltage by minimizing noise. For testing and comparison purpose, two different topologies were designed for this module. An analog multiplexing system makes it possible to activate either one or the other of the amplifiers. Another block is included in this section that is a high-pass filtering block. This block eliminates the DC component (ambient light) and adjusts the common mode voltage to a preset value.

Privileged architectures of CMOS optical preamplifiers are adapted from [7]. The first topology is a fully differential two-stage voltage operational amplifier. The second topology is a single input, single output current amplifier. However, modifications were made to allow the use of a p-substrate anode photodiode, a constraint of the used manufacturing process. The size of the transistors obviously had to be changed to meet the constraints related to scaling (from 0.35 µm to 0.18 µm), noise, gain, bandwidth and power consumption.

2.2.1. Fully differential voltage operational amplifier. This is a fixed gain fully differential transimpedance. The input transistors are of PMOS type to help decrease the input noise. Moreover, their relatively high dimensions (12x8µ/0.5µ) make them very good at rejecting 1/f noise. A significant improvement has been made compared to Phang's design as we get 1 pA / $\sqrt{\mathrm{Hz}}$ equivalent input-referred noise at 50 kHz compared to at least 13 pA / $\sqrt{\mathrm{Hz}}$.

The structure of this preamplifier is divided into two stages. The first one is a transconductance stage with gain g_{m1}. The second stage is a transresistance with gain approximately given by its resistance R_1. The open-loop gain of the complete preamplifier is thus given by:

$$A_v = \frac{v_{out+}}{v_{in-}} \approx g_{m1} R_1 \,. \tag{2}$$

As g_{m1} is 1 mS and R_1 is 10 kΩ, this gain is approximately 10 V/V. By closing the loop with a resistance R_f, the transimpedance gain of the complete preamplifier is given by :

$$R_m = \frac{v_{out+} - v_{out-}}{i_s} = \frac{A_v}{A_v + 1} R_f \,. \tag{3}$$

Since the preamplifier is the first stage of the system, it is very important to obtain a large gain in order to minimize the equivalent input noise. An A_v gain of 10 V/V is given by equation (3). It is required to maximize the value of R_f to obtain the needed transimpedance gain.

In addition, dominant pole is determined by the value of the photodiode junction capacitance (C_D) and the input resistance, which corresponds to R_f:

$$\omega_1 = \frac{1}{R_f C_D} \,. \tag{4}$$

According to equations (3) and (4), the value of R_f must be selected by making a compromise between a high gain and a high cut-off frequency. R_f was maximized to 80 kΩ in order to facilitate its integration.

The power consumption of this preamplifier was reduced from 1 mW to 0,3 mW compared to results obtained by Phang. Biasing current was kept relatively high in order to meet good noise performance.

2.2.2. Current amplifier. The designed current amplifier inspired from [7], was improved using a cascode topology and a PMOS input. It is a current mirror with a gain ratio of 2:16. The input PMOS transistors were carefully scaled in order to reduce the noise at the frequency of interest to the same level as the voltage amplifier described earlier.

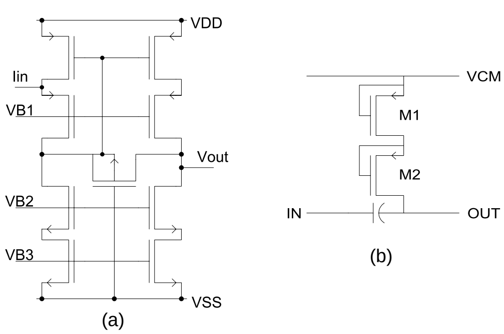

Fig. 2. (a) Current amplifier circuit and (b) HP filtering and CM voltage fixing circuit

Feedback is made by a PMOS transistor biased in the triode region and dimensioned to obtain a gain comparable to the one of the voltage amplifier topology. This current amplifier topology (fig. 2a) offers a wider bandwidth (500 kHz) than the voltage topology (80 kHz). Low input impedance of this architecture is the main factor influencing this parameter.

2.3. HP filter and common mode voltage fixing

The circuit of figure 2b, originally proposed by [8] for the high-pass filtering and common mode (CM) voltage fixing, has been used between each amplifier stage.

It acts as a RC circuit whose time-constant is very high. Indeed, the series capacitor sees a parallel resistance of several MΩ made with the two diode-connected transistors. The size of the capacitor could be minimized to 200 fF, thus saving valuable space on silicon. The cut-off frequency is difficult to predict because it is given by the value of the leakage resistance of the diode connected transistors. It is also influenced by process variations and temperature. However, worst case simulations give high-pass cut-off frequencies well less than 100 Hz. This is appropriate for this application whose band of interest is around 50 kHz. In this way, it is cutting the unwanted signals resulting from the ambient light.

On the other hand, when the output is connected to CMOS gates, the DC voltage can be set at the voltage present on the upper rail, VCM in this case.

2.4. Post-amplifiers

The front-end circuit includes two post-amplification stages, each one having a nominal voltage gain of 25 dB. An external control allows ±10 dB gain adjustment. Figure 3 illustrates the diagram of one post-amplification stage. It is composed of two unity gain buffers (UGB), a differential amplifier and two CM regulation blocks similar to those presented in figure 2b.

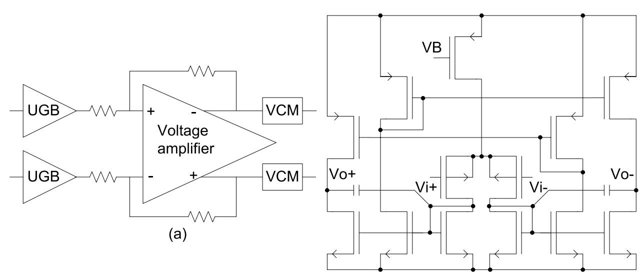

Fig. 3. Post-amplification stage (a) block diagram and (b) voltage amplifier schematic.

UGBs are used as impedance matching blocks only. The amplification element is a fully differential two-stage operational transconductance amplifier (OTA) adapted from [9]. Internal compensation had to be added because of the resistive nature of feedback. In this case, a 1.2 pF capacitor makes the phase margin vary from 20° (unstable) to more than 90° (very stable).

It is important to note that the front-end circuit allows bypassing one of the two post-amplification stages using a network transmission gates, thus optionally decreasing the total gain by 25 dB. This can be used to avoid saturation of the mixer in case of a strong input signal.

2.5. Analog Mixer

The mixer circuit is used in this system as a demodulator. This fully differential circuit consists of analog translinear multipliers. Adopted architecture is a voltage mode version of the one proposed in [10].

This mixer makes the four-quadrant analog multiplication of two differential input signals. The first input is fed by the signal coming from the amplification chain. The second input is the modulation signal provided by the emitter. The obtained continuous voltage is externally filtered and digitalized. It contains the information useful for the calculation of the variations of optical parameters on the surface of the cerebral cortex.

3. Post-Layout Simulation Results

The proposed circuit was completely characterized by simulation and implemented using TSMC 0.18 µm / 1.8 V CMOS technology. The chip is now in fabrication and test results will be available soon. Table 1 and figure 4 present the most important post-layout characteristics and simulated performances of the front-end.

Table 1. Front-End Performances

Parameter	Value
Technology	TSMC CMOS 0.18 µm N-Well
Supply voltage	1.8 V
Total silicon area	750 µm x 1600 µm
Photodetector area	448 000 μm^2
PD junction capacitance	< 4 pF
Operating frequency	1-75 kHz
Total transimpedance gain	110 to 165 dBΩ
Input current	0.2 nA to 200 nA p-p
Input refered noise	1 pA / $\sqrt{Hz}$ @ 50 kHz

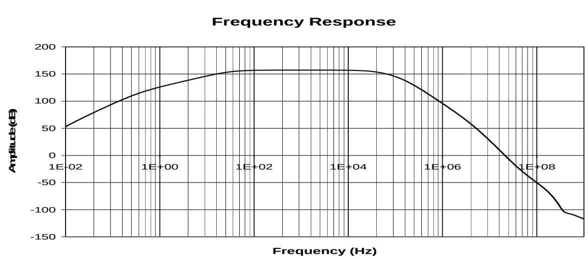

Fig. 4. Frequency response of the complete system

Care has been taken to minimize the size of the amplification circuitry to give the maximum area to the photodetector. Indeed, the photodiode covers almost all the unused space on the chip. Connection to an external photodetector is still possible, but some limitation of the bandwidth is expected due to the parasitic capacitance of an input pad. Figure 5 presents the complete circuit layout as submitted for fabrication.

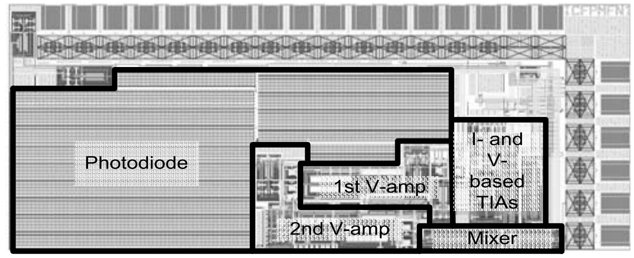

Fig. 5. Complete circuit layout

4. Conclusions

We described an optical front-end composed of a 0.45 mm^2 photodiode, a low-noise transimpedance pre-amplifier, a two-stage voltage amplifier and a mixer. The preamplifier operates at 1.8 V, has a gain of 95 dBΩ and an input-refered noise of 1 pA / $\sqrt{Hz}$ @ 50 kHz. Further stages of voltage amplification allow a total transimpedance gain of 165 dBΩ. The circuit was optimized to operate from 1 kHz to 75 kHz.

Also, the technology scaling carried out in this circuit is an important contribution for this type of application as low-voltage and low-power characteristics are now premium considerations. These good performances open the way to the design of reduced size electro-optical integrated circuits and low power consumption for portable biomedical applications.

Acknowledgements

The authors want to acknowledge financial support from NSERC and development tools and mfg services from CMC. Also, thanks are allowed to D. Morin and B. Gosselin for their inputs during layout implementation.

References

[1] Biomedical Optics Research Group, University College London, UK.
[2] Jöbsis, F.F. [1977] « Non-invasive infrared monitoring of cerebral and myocardial oxygen and circulatory parameters » *Science*, 198, 1264-1267.
[3] Wang, L.-H., Jacques, S.L. & Zheng, L.-Q. [1996] « MCML – Monte Carlo modeling of photon transport in multi-layered tissues ». *Computer Methods and Programs in Biomedicine*, 47, 131–146.
[4] Cheong, W.F., Prahl, S.A. & Welch, A.J. [1990] « A review of the optical properties of biological tissues », *IEEE Journal of Quantum Electronics*, 26, 2166–2185.
[5] Yaroslavsky, A.N., et *al*. [2002] « Optical properties of selected native and coagulated human brain tissues in vitro in the visible and near infrared spectral range », *Phys. Med. Biol*, 47(12), 2059–2073.
[6] Maciejko, R. [2002] *Optoélectonique*, Presses Polytechnique, 528 p.
[7] Phang, K. [2001] « CMOS Optical Preamplifier Design Using Graphical Circuit Analysis », 176 p. PhD. thesis, Department of Electrical and Computer Engineering, University of Toronto.
[8] Harrison, R.R., Charles, C. [2003] « A Low-Power Low-Noise CMOS Amplifier for Neural Recording Applications ». *IEEE Journal of Solid-State Circuits*, Vol 36, No. 6, 958-965.
[9] Allen, P.E. & Holberg, D.R. [2002]. *CMOS Analog Circuit Design, Second Edition*. Oxford University Press, 784 p.
[10] Johns, D.A. & Martin, K. [1997]. *Analog Integrated Circuit Design*. John Wiley & Sons, Inc., 706 p.